Probability distribution for non-Gaussianity estimators constructed from the CMB trispectrum

Tristan L. Smith and Marc Kamionkowski

Phys. Rev. D **86**, 063009 — Published 12 September 2012

DOI: 10.1103/PhysRevD.86.063009

The probability distribution for non-Gaussianity estimators constructed from the CMB trispectrum

Tristan L. Smith[1,2] and Marc Kamionkowski[3,4]

[1] *Berkeley Center for Cosmological Physics, Physics Department, University of California, Berkeley, CA 94720*
[2] *IPMU, University of Tokyo, 5-1-5 Kashiwanoha, Kashiwa, Chiba 277-8583, Japan*
[3] *California Institute of Technology, Mail Code 350-17, Pasadena, CA 91125*
[4] *Department of Physics and Astronomy, Johns Hopkins University, Baltimore, MD 21218, USA*

Considerable recent attention has focussed on the prospects to use the cosmic microwave background (CMB) trispectrum to probe the physics of the early universe. Here we evaluate the probability distribution function (PDF) for the standard estimator $\widehat{\tau_{\rm nl}}$ for the amplitude $\tau_{\rm nl}$ of the CMB trispectrum both for the null-hypothesis (i.e., for Gaussian maps with $\tau_{\rm nl}=0$) and for maps with a non-vanishing trispectrum ($\tau_{\rm nl}\neq 0$). We find these PDFs to be *highly* non-Gaussian in both cases. We also evaluate the variance with which the trispectrum amplitude can be measured, $\langle \Delta\widehat{\tau}^2_{\rm nl}\rangle$, as a function of its underlying value, $\tau_{\rm nl}$. We find a strong dependence of this variance on $\tau_{\rm nl}$. We also find that the variance does not, given the highly non-Gaussian nature of the PDF, effectively characterize the distribution. Detailed knowledge of these PDFs will therefore be imperative in order to properly interpret the implications of any given trispectrum measurement. For example, if a CMB experiment with a maximum multipole of $l_{\rm max}=1500$ (such as the Planck satellite) measures $\widehat{\tau_{\rm nl}}=0$ then at the 95% confidence our calculations show that we can conclude $\tau_{\rm nl}\leq 1005$; assuming a Gaussian PDF but with the correct $\tau_{\rm nl}$-dependent variance we would incorrectly conclude $\tau_{\rm nl}\leq 4225$; further neglecting the $\tau_{\rm nl}$-dependence in the variance we would incorrectly conclude $\tau_{\rm nl}\leq 361$.

PACS numbers:

I. INTRODUCTION

Current observations of the cosmic microwave background (CMB) and large-scale structure (LSS) provide a powerful probe of the physics of the early universe. As an example, the near scale-invariance of the primordial power-spectrum along with an upper limit to the inflationary gravitational-wave background can be used to rule out a few of the simplest models of inflation [1]. A measurement of the statistics of the primordial perturbations can provide an even more discriminating test of models of the early universe: *all* canonical single-field slow-roll inflation models predict that the perturbations are observationally indistinguishable from Gaussian [2, 3]. Therefore any observed deviation from Gaussianity will rule out all canonical single-field slow-roll inflation models. However, non-canonical single-field models [4], multi-field models [5], curvaton models [6], and models with sharp features [7] or wiggles [8] may produce larger departures from Gausianity. Measurement of the level of primordial non-Gaussianity has thus become one of the primary goals of CMB and LSS research.

The majority of efforts to measure primordial non-Gaussianity from the CMB have relied on an estimator constructed from the bispectrum, the three-point correlation function in harmonic space [9]. However, most models that predict a significant level of non-Gaussianity also predict a non-zero connected trispectrum (the non-Gaussian part of the harmonic-space four-point function) [10–15], and some efforts have been mounted to detect a primordial non-Gaussian signature from the trispectrum [10, 13, 16]. In this way a constraint on the trispectrum amplitude provides unique information on a broad range of early-universe processes such as multi-field inflation models [17], the curvaton senario [18], inflation models with non-standard kinetic terms [19], and the influence of primordial cosmic strings [20].

The level of non-Gaussianity is often quantified using the 'local-model' through the non-Gaussianity parameter $f_{\rm nl}$ defined by [9],

$$\Phi(\vec{x}) = \phi(\vec{x}) + f_{\rm nl}\left[\phi(\vec{x})^2 - \left\langle\phi^2\right\rangle\right], \qquad (1)$$

where $\Phi(\vec{x})$ is the curvature potential and $\phi(\vec{x})$ a Gaussian random field. Current limits from the CMB/LSS constrain the value to be $|f_{\rm nl}|\lesssim 80$ at 95% confidence level (c.l.) [21, 22]. The Planck satellite [23] is expected to achieve a sensitivity of $f_{\rm nl}\sim 5$.

Constraints on the amplitude of the non-Gaussian local-model CMB bispectrum and trispectrum have very broad implications. Although various physical processes predict a range of values for $f_{\rm nl}$, it can be shown that *all* single-field models of inflation predict [24]

$$f_{\rm nl} = \frac{1}{4}(n_s - 1), \qquad (2)$$

where n_s is the slope of the primordial power spectrum. Current constraints to n_s [25] imply that all single-field models predict $f_{\rm nl}\simeq -0.008$. Therefore, if the Planck satellite constrains $f_{\rm nl}$ to be non-zero, we will be able to make the profound statement that all single-field models are disfavored by the data. A measurement of the ampli-

tude of the local-model trispectrum[1], $\tau_{\rm nl}$, may lead to an additional test of the basic cosmological model. Recently Ref. [26] has shown that $\tau_{\rm nl}$ respects the inequality

$$\tau_{\rm nl} \geq \frac{1}{2}(f_{\rm nl})^2, \tag{3}$$

independent of the underlying physics. A constraint on both $f_{\rm nl}$ and $\tau_{\rm nl}$ using the CMB may appear to violate Eq. (3) at the expense of actually violating translation invariance [26]. Therefore, a constraint on both $f_{\rm nl}$ and $\tau_{\rm nl}$ provides a very broad test of some of the fundamental assumptions in our standard cosmological model. Given the wide-ranging impact of constraints on $f_{\rm nl}$ and $\tau_{\rm nl}$, it is of great importance to report the significance of any constraint accurately.

To date, most studies which use CMB observations to place constraints on $f_{\rm nl}$ and $\tau_{\rm nl}$ have used estimators that are constructed to have the minimum variance under the null hypothesis [11, 12, 27]. In order to use these estimators to place meaningful constraints on $f_{\rm nl}$ and $\tau_{\rm nl}$ we must know the full shape of their probability distribution functions (PDFs) as a function of $f_{\rm nl}$, $\tau_{\rm nl}$, and the maximum multipole $l_{\rm max}$ of the observation. Thus, for example, we often evaluate or forecast the standard error σ with which a given measurement will recover the true value of $f_{\rm nl}$ and $\tau_{\rm nl}$ and then simply assume that the error is Gaussian. If so, then with $\sigma_{\tau_{\rm nl}} = 100$, for example, a measurement of $\widehat{\tau_{\rm nl}} = 300$ would represent a 3σ departure from $\tau_{\rm nl} = 0$, and a measurement $\widehat{\tau_{\rm nl}} = 0$ would represent a 3σ departure fom $\tau_{\rm nl} = 300$. However, if the PDF depends on the true value $\tau_{\rm nl}$, and if that distribution is non-Gaussian, then it may be that a measurement $\widehat{\tau_{\rm nl}} = 300$ could be easily consistent with a true value $\tau_{\rm nl} = 0$, while a measurement $\widehat{\tau_{\rm nl}} = 0$ could be inconsistent with $\tau_{\rm nl} = 300$ with a confidence greater than "3σ." We will see below that something like this occurs with measurements of $\tau_{\rm nl}$.

A calculation of these PDFs is particularly important for measurements of non-Gaussianity (as opposed, for example, for the CMB power spectrum), because the estimator is a sum over products of three (in the case of $\widehat{f_{\rm nl}}$) or four (in the case of $\widehat{\tau_{\rm nl}}$) temperature measurements. This is unlike the power spectrum which sums over squares of temperature measurements. Suppose the temperature is measured in $N_{\rm pix}$ pixels. There are then $\sim N_{\rm pix}^2$ terms in the $f_{\rm nl}$ estimator and $\sim N_{\rm pix}^3$ terms in the $\tau_{\rm nl}$ estimator (after restrictions imposed by statistical isotropy). While these terms may have zero covariance, they are not statistically independent; there is no way to construct $N_{\rm pix}^2$ or $N_{\rm pix}^3$ statistically independent quantities from $N_{\rm pix}$ measurements. The conditions required for the validity of the central-limit theorem are therefore not met, and the estimators will not necessarily approach a Gaussian in the $N_{\rm pix} \gg 1$ limit.

Although previous studies have calculated the PDF in the case of $f_{\rm nl}$ [28, 29], the only property of the $\tau_{\rm nl}$ estimator that has been explored in the literature is how the variance for the null-case scales with the maximum observed multipole, $l_{\rm max}$ [12, 14, 16]. In order to address how well CMB observations can estimate $\tau_{\rm nl}$ we calculate the PDF $P[\widehat{\tau_{\rm nl}}; \tau_{\rm nl}, l_{\rm max}]$—the probability that a given measurement with resolution $l_{\rm max}$ will return a value $\widehat{\tau_{\rm nl}}$ given that the underlying theory has a value $\tau_{\rm nl}$—using numerous Monte Carlo realizations of an ideal (no-noise) flat-sky map in the Sachs-Wolfe approximation. In order to both generate the maps and apply the estimator to them we use a fast-Fourier transform (FFT) algorithm described in Appendix A of Ref. [29]. Lessons learned about $P[\widehat{\tau_{\rm nl}}; \tau_{\rm nl}, l_{\rm max}]$ in this ideal case help to interpret and understand current/forthcoming results and assess the validity of full-experiment simulations.

Our simulations show that $P[\widehat{\tau_{\rm nl}}; \tau_{\rm nl}, l_{\rm max}]$ is highly non-Gaussian for all values of $\tau_{\rm nl}$, including the null case. Additionally, our simulations allow us to derive, for the first time, how the variance of this distribution depends on the underlying value of $\tau_{\rm nl}$. Neglecting this dependence, Ref. [14] concludes that the signal-to-noise[2] of this estimator appears to scale as ${\tau_{\rm nl}}^2$, becoming more sensitive to non-Gaussianity for large $\tau_{\rm nl}$ than an estimator using the CMB bispectrum. We show that the dependence of the variance on the underlying value of $\tau_{\rm nl}$ is significant, finding that the sensitivity of this estimator to local-model non-Gaussianity is always weaker than that of the bispectrum estimator, and it approaches a constant for $\tau_{\rm nl} \gtrsim 10^9/l_{\rm max}^2$.

Knowledge of both the variance and shape of $P[\widehat{\tau_{\rm nl}}; \tau_{\rm nl}, l_{\rm max}]$ is necessary to assign proper confidence levels (c.l.) to constraints. For example, if the Planck satellite ($l_{\rm max} \simeq 1500$) measures $\widehat{\tau_{\rm nl}} = 0$ then at the 95% c.l. our calculations show that we can conclude $\tau_{\rm nl} \leq 1005$. If we assumed a Gaussian PDF but with the correct $\tau_{\rm nl}$-dependent variance we would incorrectly conclude $\tau_{\rm nl} \leq 4225$. If we also neglected to include the $\tau_{\rm nl}$-dependent variance we would incorrectly conclude $\tau_{\rm nl} \leq 361$.

This paper is organized as follows. In Sec. II, we discuss how to construct the minimum-variance estimator $\widehat{\tau_{\rm nl}}$ using the CMB trispectrum under the null-hypothesis. In Sec. III we apply this estimator to the local-model for non-Gaussianity. In Sec. III A we present our results for the PDF in the null ($\tau_{\rm nl} = 0$) case. Sec. III B presents our results for the non-null case and gives a fitting formula

[1] The local-model trispectrum can be defined by using Eq. (1) with the identification $\tau_{\rm nl} = {f_{\rm nl}}^2$.

[2] The signal-to-noise is defined to be $S/N \equiv \tau_{\rm nl}/\sigma_{\tau_{\rm nl}}$. In the case of Gaussian noise with a variance independent of $\tau_{\rm nl}$ this is a measure of the fractional error in a constraint to $\tau_{\rm nl}$. However, in the case of $\widehat{\tau_{\rm nl}}$, the noise is neither Gaussian nor independent of $\tau_{\rm nl}$ so that the quantity $\tau_{\rm nl}/\sigma_{\tau_{\rm nl}}$ is only an approximation to the significance of a constraint on $\tau_{\rm nl}$.

for $P[\widehat{\tau_{\rm nl}};\tau_{\rm nl},l_{\rm max}]$. In Sec. IV we summarize our results.

II. NON-GAUSSIANITY ESTIMATORS CONSTRUCTED FROM THE CMB TRISPECTRUM

A. Formalism

We assume a flat sky to avoid the complications (e.g., spherical harmonics, Clebsch-Gordan coefficients, Wigner $3j$ and $6j$ symbols, etc.) associated with a spherical sky, and we further assume the Sachs-Wolfe limit. We denote the fractional temperature perturbation at position $\vec{\theta}$ on a flat sky by $T(\vec{\theta})$ and refer to it hereafter simply as the temperature.

The field $T(\vec{\theta})$ has a power spectrum C_l given by

$$\left\langle T_{\vec{l}_1} T_{\vec{l}_2} \right\rangle = \Omega \delta_{\vec{l}_1+\vec{l}_2,0} C_l, \tag{4}$$

where $\Omega = 4\pi f_{\rm sky}$ is the survey area (in steradians),

$$T_{\vec{l}} = \int d^2\vec{\theta}\, e^{-i\vec{l}\cdot\vec{\theta}} T(\vec{\theta}) \simeq \frac{\Omega}{N_{\rm pix}} \sum_{\vec{\theta}} e^{-i\vec{l}\cdot\vec{\theta}} T(\vec{\theta}), \tag{5}$$

is the Fourier transform of $T(\vec{\theta})$, and $\delta_{\vec{l}_1+\vec{l}_2,0}$ is a Kronecker delta that sets $\vec{l}_1 = -\vec{l}_2$. In the limit of small departures from Gaussianity, C_l is also the power spectrum for $T(\vec{\theta})$, which for a scale-invariant primordial power spectrum with amplitude A ($A \simeq 10^{-10}$) is given by

$$C_l = \frac{2\pi A}{l^2}. \tag{6}$$

The trispectrum is defined by [11, 12]

$$\left\langle T_{\vec{l}_1} T_{\vec{l}_2} T_{\vec{l}_3} T_{\vec{l}_4} \right\rangle = \tau_{\rm nl} \Omega \delta_{\vec{l}_1+\vec{l}_2+\vec{l}_3+\vec{l}_4,0} \mathcal{T}(\vec{l}_1,\vec{l}_2,\vec{l}_3,\vec{l}_4), \tag{7}$$

and for the local-model,

$$\begin{aligned} \mathcal{T}(\vec{l}_1,\vec{l}_2,\vec{l}_3,\vec{l}_4) &= P^{l_1 l_2}_{l_3 l_4}(|\vec{l}_1+\vec{l}_2|). \\ &+ P^{l_1 l_3}_{l_2 l_4}(|\vec{l}_1+\vec{l}_3|) + P^{l_1 l_4}_{l_2 l_3}(|\vec{l}_1+\vec{l}_4|), \end{aligned} \tag{8}$$

where

$$\begin{aligned} P^{l_1 l_2}_{l_3 l_4}(|\vec{l}_1+\vec{l}_2|) &\equiv 4 C_{|\vec{l}_1+\vec{l}_2|} \left[C_{l_1} C_{l_3} + C_{l_1} C_{l_4} \right. \\ &\left. + C_{l_2} C_{l_3} + C_{l_2} C_{l_4} \right]. \end{aligned} \tag{9}$$

Due to statistical isotropy, the trispectrum is nonvanishing only for $\vec{l}_1+\vec{l}_2+\vec{l}_3+\vec{l}_4 = 0$, that is, only for quadrilaterals in Fourier space.

B. The minimum-variance trispectrum estimator

Each distinct quadrilateral $\vec{l}_1+\vec{l}_2+\vec{l}_3+\vec{l}_4 = 0$ gives an estimator for the trispectrum with some variance. Adding the individual estimators with inverse-variance weighting gives the minimum-variance estimator,

$$\begin{aligned} \widehat{\tau_{\rm nl}} &= \sigma^2_{T,0} \sum_{\vec{l}_1+\vec{l}_2+\vec{l}_3+\vec{l}_4=0} \frac{T_{\vec{l}_1} T_{\vec{l}_2} T_{\vec{l}_3} T_{\vec{l}_4}}{4! \Omega^3 C_{l_1} C_{l_2} C_{l_3} C_{l_4}} \\ &\times \mathcal{T}(\vec{l}_1,\vec{l}_2,\vec{l}_3,\vec{l}_4) - \sigma^2_{T,0} \left\langle \mathcal{T} \right\rangle_G, \end{aligned} \tag{10}$$

where we have subtracted off the unconnected (Gaussian) part of the trispectrum, $\langle \mathcal{T} \rangle_G$, and the inverse variance is given by

$$\sigma^{-2}_{T,0} = \sum_{\vec{l}_1+\vec{l}_2+\vec{l}_3+\vec{l}_4=0} \frac{\left[\mathcal{T}(\vec{l}_1,\vec{l}_2,\vec{l}_3,\vec{l}_4) \right]^2}{4! \Omega^2 C_{l_1} C_{l_2} C_{l_3} C_{l_4}}, \tag{11}$$

where $2 \le |\vec{l}_i| \le l_{\rm max}$.

III. THE PDF OF $\widehat{\tau_{\rm nl}}$ FOR THE LOCAL-MODEL

We now restrict our attention to the local family of non-Gaussian models [see Eq. (1)] in which the temperature $T(\vec{\theta})$ has a non-Gaussian component,

$$T(\vec{\theta}) = t(\vec{\theta}) + 3\sqrt{\tau_{\rm nl}} \left\{ [t(\vec{\theta})]^2 - \left\langle [t(\vec{\theta})]^2 \right\rangle \right\}, \tag{12}$$

where we have chosen the normalization $\tau_{\rm nl}$ to correspond to amplitude of the non-Gaussian part of the Newtonian potential four-point function[3]. To zeroth order in $\tau_{\rm nl}$, the power spectrum and correlation function for $T(\vec{\theta})$ are the same as those for $t(\vec{\theta})$. Note that $T(\vec{\theta})$ is, strictly speaking, the temperature fluctuation, so $\left\langle T(\vec{\theta}) \right\rangle = 0 = T_{\vec{l}=0}$.

The temperature Fourier coefficients can be written $T_{\vec{l}} = t_{\vec{l}} + \sqrt{\tau_{\rm nl}} \delta t^2_{\vec{l}}$ with

$$\delta t^2_{\vec{l}} \equiv \frac{3}{\Omega} \sum_{\vec{l}_1+\vec{l}_2=\vec{l}} t_{\vec{l}_1} t_{\vec{l}_2}. \tag{13}$$

Formally, the sum goes from $1 \le |\vec{l}_1| < \infty$, but for a finite-resolution map, the sum is truncated at some $l_{\rm max}$ such that the number of Fourier modes equals the number of data points.

Applying the estimator in Eq. (10) to the local-model trispectrum [Eq. (8)], we obtain

$$\widehat{\tau_{\rm nl}} = 2 \sum_{1 \le |\vec{L}| \le 2l_{\rm max}} C_L \left| \sum_{\vec{l}_1+\vec{l}_2+\vec{L}=0} \frac{T_{\vec{l}_1} T_{\vec{l}_2}}{\Omega^2 C_{l_1}} \right|^2 - \sigma^2_{T,0} \left\langle \mathcal{T} \right\rangle_G \tag{14}$$

[3] This differs by a factor of 5/6 the usual definition which is given in terms of the Bardeen potential [30].

where we can now write

$$\langle \mathcal{T} \rangle_G = 2\sigma_{T,0}^2 \sum_{|\vec{L}|>1} C_L \sum_{\vec{l}_1+\vec{l}_2+\vec{L}=0} \left(\frac{C_{l_1}}{C_{l_2}} + 1 \right). \qquad (15)$$

A. The PDF of $\widehat{\tau_{\rm nl}}$ under the null-hypothesis, $\tau_{\rm nl} = 0$

Under the null hypothesis ($\tau_{\rm nl} = 0$) we apply $\widehat{\tau_{\rm nl}}$ to a purely Gaussian CMB temperature map. As shown in

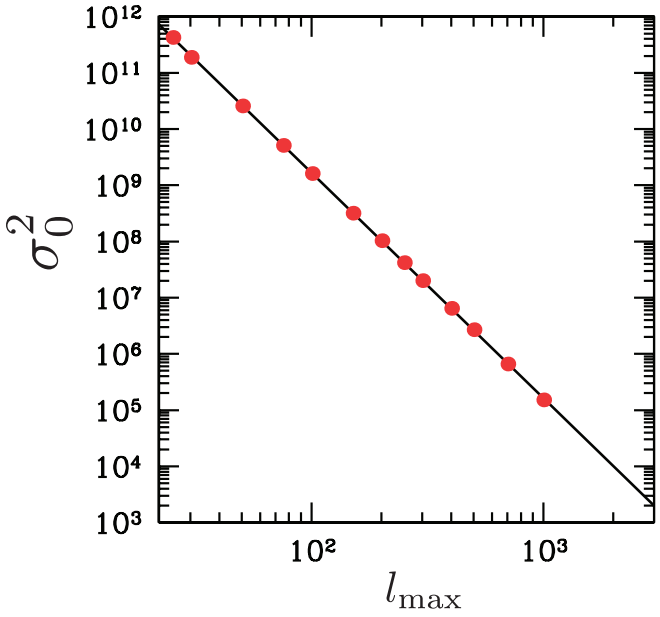

FIG. 1: The scaling of the variance of $\widehat{\tau_{\rm nl}}$ under the null hypothesis $\tau_{\rm nl} = 0$. Each red point shows the result of a Monte Carlo simulation for 1000 realizations. The black line is a fit to those simulations given by Eq. (16).

Fig. 1, our Monte Carlo simulations find that the variance σ_0 of this estimator under the null hypothesis as a function of the maximum multipole $l_{\rm max}$ included in the analysis is well-fit by a power-law

$$\sigma_0^2(l_{\rm max}) = \frac{1.74 \times 10^{-2}}{A^2 {l_{\rm max}}^4}. \qquad (16)$$

This scaling compares well with the results of previous work [12, 14].

The simulations also allow us to calculate the full shape of the PDF of this estimator under the null hypothesis. Since the number $N_{\rm pix}$ of measurements of the CMB temperature map is much less than the number ($\sim N_{\rm pix}^3$) of terms in this estimator, the standard central-limit theorem does not apply so that the PDF $P[\widehat{\tau_{\rm nl}}; \tau_{\rm nl} = 0, l_{\rm max}]$, is not necessarily Gaussian in the $N_{\rm pix} \gg 1$ limit. The simulations demonstrate that the PDF is, in fact, highly non-Gaussian as shown in Fig. 2. The asymmetry of the PDF can be explained by referring to the expression for the estimator in Eq. (14). There it can be seen that the estimator is bounded from below but unbounded from above. By calculating the PDF, $P[\widehat{\tau_{\rm nl}}; \tau_{\rm nl} = 0, l_{\rm max}]$, for

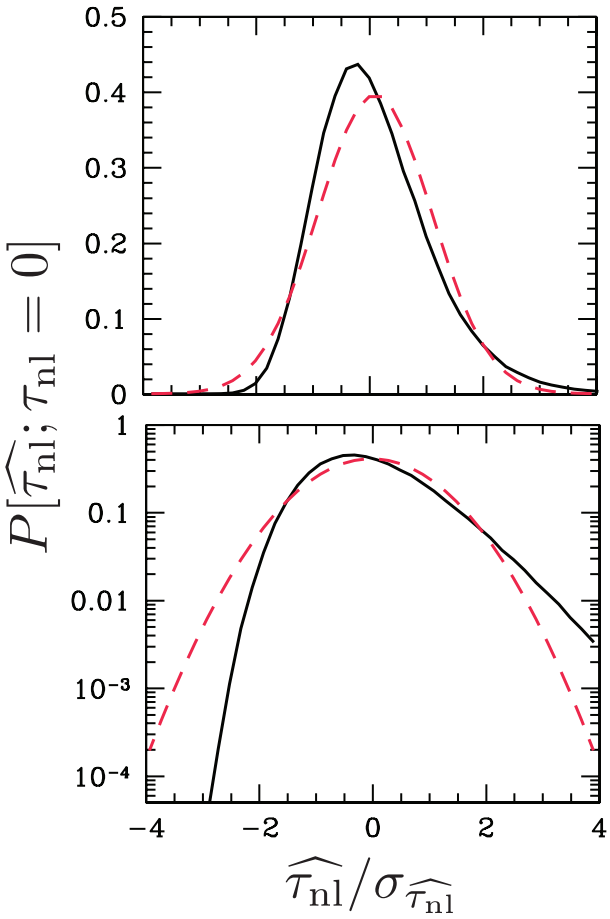

FIG. 2: The black-solid curve shows the PDF of $\widehat{\tau_{\rm nl}}$ under the null-hypothesis, $\tau_{\rm nl} = 0$ for $l_{\rm max} = 50$ and calculated with 10^6 realizations. The red-dashed curve shows a Gaussian PDF with the same variance. The upper panel shows the PDF on a linear scale, the low panel on a logarithmic scale. When scaled by its variance, the PDF is identical for $l_{\rm max} = 100$ showing that it takes on a universal form in the $l_{\rm max} \gg 1$ limit. We give a fitting formula for this PDF in Eq. (17).

several values of $l_{\rm max}$ we find that when scaled by its variance it takes on the universal shape shown by the black curve in Fig. 2. The PDF is well fit by the formula,

$$P[\widehat{\tau_{\rm nl}}; \tau_{\rm nl} = 0, l_{\rm max}] = \frac{1}{\sigma N} \qquad (17)$$
$$\begin{cases} e^{-\frac{1}{2}\left|\frac{\widehat{\tau_{\rm nl}}/\sigma - x_p}{\sigma_p}\right|^n}, & \widehat{\tau_{\rm nl}}/\sigma \le x_p, \\ e^{-\frac{c}{\sigma_p^2}\left(\sqrt{(\widehat{\tau_{\rm nl}}/\sigma - x_p)^2 + c^2} - c\right)}, & \widehat{\tau_{\rm nl}}/\sigma > x_p, \end{cases}$$

where σ is the variance of the estimator, given in Eq. (16), the normalization N is given by

$$N \equiv 2\sigma_p \Gamma\left(\frac{n+1}{n}\right) + c\, e^{c^2/\sigma_p^2} K_1\left(\frac{c^2}{\sigma_p^2}\right), \qquad (18)$$

where Γ is the Euler Gamma function, and K_1 is the modified Bessel function of the first kind. We find that

the PDF is best fit by the parameters $n = 3$, $x_p = -0.13$, $\sigma_p = 0.64$, and $c = 0.488$.

B. The PDF of $\widehat{\tau_{\rm nl}}$ with $\tau_{\rm nl} \neq 0$

For $\tau_{\rm nl} \neq 0$ the non-Gaussianity in the CMB map imparts further non-Gaussianity to the shape of $P[\widehat{\tau_{\rm nl}}; \tau_{\rm nl}, l_{\rm max}]$. In addition to this, the variance has a strong dependence on $\tau_{\rm nl}$ so that when $\tau_{\rm nl}$ and $l_{\rm max}$ are large enough the ratio $\tau_{\rm nl}/\sigma_{\tau_{\rm nl}}$, which approximates the S/N of the estimator, approaches a constant value.

In order to investigate how the variance of $\widehat{\tau_{\rm nl}}$ depends on $\tau_{\rm nl}$ it is useful to expand it in powers of $\tau_{\rm nl}$. Given that T_l is linear in $\tau_{\rm nl}$ and that $\widehat{\tau_{\rm nl}}$ is quartic in T_l the expansion includes terms up to ${\tau_{\rm nl}}^2$:

$$\widehat{\tau_{\rm nl}} = \mathcal{T}_0 + \sqrt{\tau_{\rm nl}}\mathcal{T}_1 + \tau_{\rm nl}\mathcal{T}_2 + {\tau_{\rm nl}}^{3/2}\mathcal{T}_3 + {\tau_{\rm nl}}^2\mathcal{T}_4, \qquad (19)$$

where each $\mathcal{T}_i \sim \Sigma t_l^{i+4}$. We give explicit expressions for the $\mathcal{T}_i$ in Appendix A.

Since only cross-correlations which include even products of t are non-zero, the variance of $\widehat{\tau_{\rm nl}}$ is given by

$$\begin{aligned}\left\langle [\Delta\widehat{\tau_{\rm nl}}]^2 \right\rangle &= \sigma_0^2 + \tau_{\rm nl}(\sigma_1^2 + \sigma_{0,2}^2) \\ &+ {\tau_{\rm nl}}^2(\sigma_2^2 + \sigma_{0,4}^2 + \sigma_{1,3}^2) \\ &+ {\tau_{\rm nl}}^3(\sigma_3^2 + \sigma_{2,4}^2) + {\tau_{\rm nl}}^4\sigma_4^2,\end{aligned} \qquad (20)$$

where, for example, $\sigma_{0,2}^2$ denotes the covariance between $\mathcal{T}_0$ and $\mathcal{T}_2$ and $\Delta\widehat{\tau_{\rm nl}} \equiv \widehat{\tau_{\rm nl}} - \langle\widehat{\tau_{\rm nl}}\rangle$.

Calculating the terms that appear in Eq. (21) using Monte Carlo simulations we find that for $\tau_{\rm nl} < 10^4$ and $l_{\rm max} < 10^4$ only σ_1^2 and σ_2^2 significantly contribute. The variance is then well approximated by

$$\left\langle [\Delta\widehat{\tau_{\rm nl}}]^2 \right\rangle \approx \sigma_0^2 + \tau_{\rm nl}\sigma_1^2 + {\tau_{\rm nl}}^2\sigma_2^2, \qquad (21)$$

where σ_0^2 is given in Eq. (16) and

$$\sigma_1^2 = \frac{0.028}{A{l_{\rm max}}^2}, \qquad (22)$$

$$\sigma_2^2 = 0.23. \qquad (23)$$

The results of our Monte Carlo simulations are shown in Fig. 3.

The scaling given in Eq. (21) shows that for a large enough $l_{\rm max}$ the variance of the estimator scales as ${\tau_{\rm nl}}^2$ so that the ratio $\widehat{\tau_{\rm nl}}/\sigma_{\widehat{\tau_{\rm nl}}}$ becomes constant for $\tau_{\rm nl} \gtrsim 0.1/(A{l_{\rm max}}^2)$. A similar scaling is observed with the minimum-variance null-hypothesis estimator using the CMB bispectrum [28, 29]. Neglecting the dependence of the variance on $\tau_{\rm nl}$, previous work [14] claimed that for large enough $\tau_{\rm nl}$ the minimum-variance null-hypothesis estimator using the CMB trispectrum would be more sensitive to a local-model non-Gaussian signal than an estimator using the CMB bispectrum with the relationship $\tau_{\rm nl} = {f_{\rm nl}}^2$. Given the dependence of the variance on

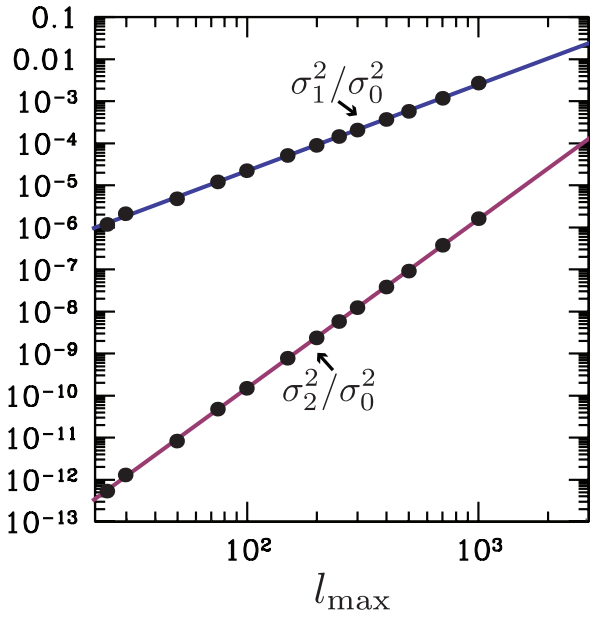

FIG. 3: The variances σ_1^2 and σ_2^2 as a fraction of the zeroth-order variance σ_0^2. The points are the results of the Monte Carlo simulations and the curves show the power-law fits given in Eqs. (22) and (23).

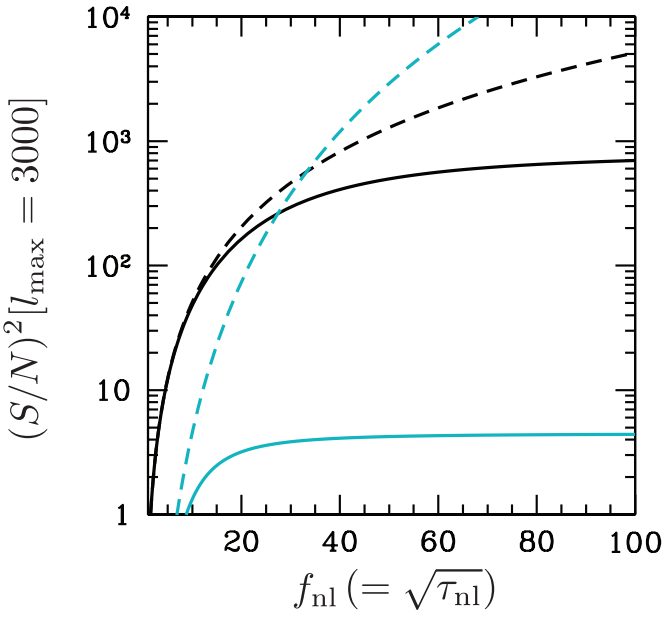

FIG. 4: The ratio ${f_{\rm nl}}^2/\sigma^2_{f_{\rm nl}}$ using the CMB bispectrum (black, from Ref. [29]) and ${\tau_{\rm nl}}^2/\sigma^2_{\tau_{\rm nl}}$ using the CMB trispectrum [blue, Eq. (21)] as a function of $\tau_{\rm nl} = {f_{\rm nl}}^2$. These ratios can be interpreted as an estimate for the S/N for a constraint to local-model non-Gaussianity in the CMB. The dashed curves show the scaling of the S/N without taking into account the dependence of the variance on $f_{\rm nl}$ and $\tau_{\rm nl}$; the solid curves show the correct S/N scaling. As in Ref. [14], from the dashed curves we would (incorrectly) conclude that the trispectrum estimator is more sensitive to a non-Gaussian signal for $\sqrt{\tau_{\rm nl}} \gtrsim 40$.

$\tau_{\rm nl}$ our calculations demonstrate that this is not the case, as shown by the solid curves in Fig. 4.

When $\widehat{\tau_{\rm nl}}$ is applied to a map with $\tau_{\rm nl} \neq 0$ then the non-Gaussianity in the map imparts additional non-Gaussianity to $P[\widehat{\tau_{\rm nl}}; \tau_{\rm nl}, l_{\rm max}]$. We are interested in calculating the shape of the PDF for an experiment such as Planck which has $l_{\rm max} \simeq 1500$. Although, in principle, it is possible calculate the PDF for large $l_{\rm max}$, it is computationally demanding especially given the large number of realizations we must generate in order to explore the tails of the distribution. The computation can be simplified since we find the PDF is 'self-similar' in the sense that its shape depends on the ratios σ_0^2/σ_1^2 and σ_0^2/σ_2^2. Given Eqs. (16), (22), and (23) this implies that the shape depends on the combination $\tau_{\rm nl} l_{\rm max}^2$.

Using this fact it is straightforward to calculate the PDF for a moderate value of $l_{\rm max}$ (we used $l_{\rm max} = 50$) and then scale the PDF to a larger value for various choices of $\tau_{\rm nl}$. We find that $P[\widehat{\tau_{\rm nl}}; \tau_{\rm nl}, l_{\rm max}]$ is well fit by the formula used to fit $P[\widehat{\tau_{\rm nl}}; \tau_{\rm nl} = 0, l_{\rm max}]$, given by Eq. (17), with parameters n, σ_p, x_p, and c which now depend on $f_{\rm nl}$ and σ is the variance of the estimator given by Eq. (21). In Fig. 5 we show how these parameters depend on $\tau_{\rm nl}$ for $l_{\rm max} = 600$ (dotted), $l_{\rm max} = 1500$ (dashed) and $l_{\rm max} = 3000$ (solid). We find that as $\tau_{\rm nl}$ increases the asymmetry of the PDF increases with the power-law index of the PDF for $\widehat{\tau_{\rm nl}} < \tau_{\rm nl}$ growing from $n = 3$ to $n = 4$ for $l_{\rm max} = 1500$ and $n = 4.24$ for $l_{\rm max} = 3000$.

Our knowledge of the full shape of $P[\widehat{\tau_{\rm nl}}; \tau_{\rm nl}, l_{\rm max}]$ now allows us to properly assign confidence levels (c.l.). If a given CMB observation with $l_{\rm max}$ yields a value of $(\widehat{\tau_{\rm nl}})_{\rm obs}$ we assign the 95% c.l. by finding the value of $(\tau_{\rm nl})_{\pm {\rm c.l.}}$ which satisfies the integral equation

$$0.95 = \left| \int_{(\widehat{\tau_{\rm nl}})_{\rm obs}}^{(\widehat{\tau_{\rm nl}})_{\pm}} P[\widehat{\tau_{\rm nl}}; (\tau_{\rm nl})_{\pm {\rm c.l.}}, l_{\rm max}] d\widehat{\tau_{\rm nl}} \right|, \qquad (24)$$

where $(\widehat{\tau_{\rm nl}})_{\pm}$ is the solution to the equation

$$P[(\widehat{\tau_{\rm nl}})_{\pm}; (\tau_{\rm nl})_{\pm {\rm c.l.}}, l_{\rm max}] = P[(\widehat{\tau_{\rm nl}})_{\rm obs}; (\tau_{\rm nl})_{\pm {\rm c.l.}}, l_{\rm max}]. \qquad (25)$$

If, for example, an experiment with $l_{\rm max} = 3000$ measures $\langle \widehat{\tau_{\rm nl}} \rangle = 100$ then at the 95% c.l., $\tau_{\rm nl} = 100^{+210}_{-64}$. If we assumed a Gaussian PDF with the $\tau_{\rm nl}$-dependent variance given by Eq. (21) we would incorrectly conclude $\tau_{\rm nl} = 100^{+3180}_{-94}$. Finally, if we also neglected to include the $\tau_{\rm nl}$-dependent variance we would incorrectly conclude $\tau_{\rm nl} = 100 \pm 92$.

IV. DISCUSSION

In this paper we have shown that the PDF for non-Gaussianity estimators using the CMB trispectrum cannot be assumed to be Gaussian, since the number, $\sim N_{\rm pix}^3$, of terms used to construct these estimators greatly exceeds the number $N_{\rm pix}$ of measurements. The 99.6% confidence-level interval cannot safely be assumed to be 3 times the 68.2% confidence-level interval. We found that the PDF of standard minimum-variance estimator $\widehat{\tau_{\rm nl}}$ using the CMB trispectrum constructed under the null hypothesis is well-approximated by a distribution given by Eqs. (17) and (21). This distribution is exponentially suppressed for values $\widehat{\tau_{\rm nl}} < \tau_{\rm nl}$ and enhanced for values $\widehat{\tau_{\rm nl}} > \tau_{\rm nl}$, relative to a Gaussian with the same variance. We calculated how the parameters of this fitting formula depend on $\tau_{\rm nl}$ for $l_{\rm max} = 600$, $l_{\rm max} = 1500$ and $l_{\rm max} = 3000$ as shown in Fig. 5. We also find that the non-Gaussianity of $P[\widehat{\tau_{\rm nl}}; \tau_{\rm nl}, l_{\rm max}]$ is greater for $\tau_{\rm nl} \neq 0$.

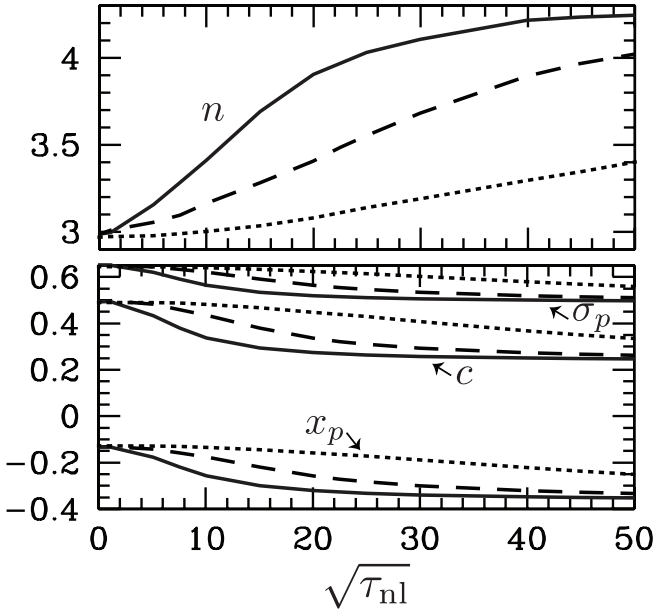

FIG. 5: The scaling of the parameters for the fitting formula in Eq. (17) with $\sqrt{\tau_{\rm nl}}$ for $l_{\rm max} = 600$ (dotted curves) $l_{\rm max} = 1500$ (dashed curves) and $l_{\rm max} = 3000$ (solid curves) . For $\tau_{\rm nl} \neq 0$ the non-Gaussianity of the map imparts additional non-Gaussianity to the PDF. As $\tau_{\rm nl}$ increases the asymmetry of the PDF increases with the power-law index of the PDF for $\widehat{\tau_{\rm nl}} < \tau_{\rm nl}$ going from $n = 3$ to $n = 4$ in the case of $l_{\rm max} = 1500$, and $n = 4.24$ in the case of $l_{\rm max} = 3000$.

We have calculated, for the first time, how the variance of $\widehat{\tau_{\rm nl}}$ depends on the underlying value of $\tau_{\rm nl}$, as shown in Eq. (21). Previous work neglected this dependence leading to the incorrect conclusion that for large enough $\tau_{\rm nl}$ and $l_{\rm max}$ a non-Gaussianity estimator constructed from the CMB trispectrum would have a larger S/N than an estimator constructed from the CMB bispectrum [14]. When the $\tau_{\rm nl}$ dependence in the variance is included the S/N of the estimator constructed from the CMB trispectrum becomes constant for $\tau_{\rm nl} > 0.1/(A l_{\rm max}^2)$. As a result, the estimator constructed from the CMB bispectrum always produces a larger S/N, as shown by the solid curves in Fig. 4.

These results have important consequences for future constraints to $\tau_{\rm nl}$ measured from the CMB. As discussed in the Introduction, future constraints to both $f_{\rm nl}$ and $\tau_{\rm nl}$ may imply wide-ranging conclusions about the physics of

the early universe. In particular, a non-zero measurement of $f_{\rm nl}$ would rule out *all* single-field inflation models and a constraint to $\tau_{\rm nl}$ probes basic physical assumptions of the early universe, such as translation invariance, by testing the consistency relation, $\tau_{\rm nl} \geq {f_{\rm nl}}^2/2$ around the surface of last scattering [24, 26]. If we suppose an experiment with $l_{\rm max} = 3000$ measures $\widehat{f_{\rm nl}} = 20$ and $\widehat{\tau_{\rm nl}} = 0$ then at the 95% c.l. our calculations show that we can conclude $\tau_{\rm nl} \leq 200$, violating the consistency relation $\tau_{\rm nl} \geq {f_{\rm nl}}^2/2$ at the 95% c.l. If we assumed a Gaussian PDF for $\widehat{\tau_{\rm nl}}$ but with the correct $\tau_{\rm nl}$-dependent variance found in Eq. (21) we would incorrectly find $\tau_{\rm nl} \leq 1000$, leading to the false conclusion that $\tau_{\rm nl} \geq {f_{\rm nl}}^2/2$ is consistent with the data. If we also neglected to include the $\tau_{\rm nl}$-dependent variance we would incorrectly find $\tau_{\rm nl} \leq 90$.

The non-Gaussian shape of the PDF of $\widehat{\tau_{\rm nl}}$ is important even for current constraints. The current published constraints on $\tau_{\rm nl}$ from the Wilkinson Microwave Anisotropy Probe (WMAP) [16, 21] ($l_{\rm max} = 600$) are $\tau_{\rm nl}/10^4 = 1.68 \pm 1.31$ at the 68% c.l. [16]. The error quoted in this constraint is estimated without taking into account the full shape of the PDF. Although our results are not directly applicable to this case since they do not take into account several details of the WMAP analysis (such as a full CMB transfer function and the noise properties of the observations) they do allow us to discuss how using the correct PDF would qualitatively change the confidence levels. For $l_{\rm max} = 600$ our calculations show that when assuming a Gaussian PDF along with a $\tau_{\rm nl}$ independent variance the constraint is $\tau_{\rm nl}/10^4 = 1 \pm 0.1$; the full PDF shows the actual constraint to be $\tau_{\rm nl}/10^4 = 1^{+1.61\ +3.3}_{-0.2\ -0.6}$. This indicates that a complete treatment of the confidence levels for the current constraint on $\tau_{\rm nl}$ is both asymmetric and has a larger range than the constraint that is quoted in Ref. [16].

The results presented here are made within the flat-sky, Sachs-Wolfe approximation. As such our conclusions should be taken as an order-of-magnitude estimate of $P[\widehat{\tau_{\rm nl}}; \tau_{\rm nl}, l_{\rm max}]$ calculated on the full sky and with the full transfer function (see Ref. [28] for a further discussion). However, we note that a comparison between the exact and approximate scaling of the S/N with $l_{\rm max}$ shows the agreement to be better than an order of magnitude [27].

In this paper we have concentrated solely on the non-Gaussian local-model, defined in Eq. (1). Although the quantitative results will differ for other models of non-Gaussianity, we expect that the qualitative conclusions will remain unchanged. The non-Gaussian PDF for $\widehat{\tau_{\rm nl}}$ results from a breakdown of the central-limit theorem due to the large number of terms used in the estimator compared to the number of independent measurements. Therefore, the work presented here shows that estimators for the CMB trispectrum amplitude cannot be assumed to have a Gaussian PDF. Rather, one must carefully explore the full shape of the PDF before assigning the significance of any particular measurement. Similar considerations may also need to be considered, for example, in measurements of things like weak gravitaitonal lensing, departures from statistical isotropy [32], and the like, as the magntiudes of many of these effects are determined in practice by the trispectrum.

Acknowledgments

TLS was supported by the Berkeley Center of Cosmological Physics and thanks the Institute for the Physics and Mathematics of the Universe (IPMU), University of Tokyo, for hospitality while this work was completed. MK was supported by DoE DE-FG03-92- ER40701 and NASA NNX12AE86G.

Appendix A: The expansion of $\widehat{\tau_{\rm nl}}$ in $\tau_{\rm nl}$

Here we write down the explicit formulas for the expansion of $\widehat{\tau_{\rm nl}}$, the minimum-variance estimator using the CMB trispectrum constructed under the null hypothesis, as written out schematically in Eq. (19). The standard estimator applied to the non-Gaussian local-model, defined by Eq. (1), can be written

$$\widehat{\tau_{\rm nl}} + \sigma^2_{T,0} \langle \mathcal{T} \rangle_G = \tag{A1}$$
$$2\sigma^4_{T,0} \sum_{|\vec{L}|=-2l_{\rm max},\ \vec{L}\neq 0}^{2l_{\rm max}} C_L \left| \sum_{\vec{l}_1+\vec{l}_2+\vec{L}=0} \frac{T_{\vec{l}_1} T_{\vec{l}_2}}{\Omega^2 C_{l_1}} \right|^2 .$$

Noting that $T_{\vec{l}} = t_{\vec{l}} + \sqrt{\tau_{\rm nl}}\delta t^2_{\vec{l}}$ we have

$$\begin{aligned}\widehat{\tau_{\rm nl}} \ &= \ 2\sigma^4_{T,0} \sum_{|\vec{L}|=-2l_{\rm max},\ \vec{L}\neq 0}^{2l_{\rm max}} C_L \Big\{ |A_1|^2 + \sqrt{\tau_{\rm nl}} \left(A_1 A_2^* + A_2 A_1^2 \right) \\ &+ \ \tau_{\rm nl} \left(|A_2|^2 + A_1 A_3^* + A_3 A_1^* \right) \\ &+ \ {\tau_{\rm nl}}^{3/2} \left(A_2 A_3^* + A_3 A_2^* \right) + {\tau_{\rm nl}}^2 |A_3|^2 \Big\} - \langle \widehat{\tau_{\rm nl}} \rangle \Big|_{\tau_{\rm nl}=0}, \end{aligned} \tag{A2}$$

where

$$A_1(\vec{L}) \ \equiv \ \sum_{\vec{l}_1+\vec{l}_2+\vec{L}=0} \frac{t_{\vec{l}_1} t_{\vec{l}_2}}{C_{l_1}}, \tag{A3}$$

$$A_2(\vec{L}) \ \equiv \ \sum_{\vec{l}_1+\vec{l}_2+\vec{L}=0} \frac{t_{\vec{l}_1} \delta t^2_{\vec{l}_2} + t_{\vec{l}_2} \delta t^2_{\vec{l}_1}}{C_{l_1}}, \tag{A4}$$

$$A_3(\vec{L}) \ \equiv \ \sum_{\vec{l}_1+\vec{l}_2+\vec{L}=0} \frac{\delta t^2_{\vec{l}_1} \delta t^2_{\vec{l}_2}}{C_{l_1}}. \tag{A5}$$

[1] F. Finelli, J. Hamann, S. M. Leach and J. Lesgourgues, JCAP **1004**, 011 (2010) [arXiv:0912.0522 [astro-ph.CO]].

[2] A. H. Guth and S. Y. Pi, Phys. Rev. Lett. **49**, 1110

(1982); A. A. Starobinsky, Phys. Lett. B **117**, 175 (1982); J. M. Bardeen, P. J. Steinhardt and M. S. Turner, Phys. Rev. D **28**, 679 (1983).

[3] T. Falk, R. Rangarajan and M. Srednicki, Astrophys. J. **403**, L1 (1993) [arXiv:astro-ph/9208001]; A. Gangui *et al.*, Astrophys. J. **430**, 447 (1994) [arXiv:astro-ph/9312033]; A. Gangui, Phys. Rev. D **50**, 3684 (1994) [arXiv:astro-ph/9406014]; J. M. Maldacena, JHEP **0305**, 013 (2003) [arXiv:astro-ph/0210603]; V. Acquaviva, N. Bartolo, S. Matarrese and A. Riotto, Nucl. Phys. B **667**, 119 (2003) [arXiv:astro-ph/0209156]; D. Babich, P. Creminelli and M. Zaldarriaga, JCAP **0408**, 009 (2004) [arXiv:astro-ph/0405356]; P. Creminelli *et al.*, JCAP **0605**, 004 (2006) [arXiv:astro-ph/0509029]; P. Creminelli *et al.*, JCAP **0703**, 005 (2007) [arXiv:astro-ph/0610600].

[4] C. Armendariz-Picon, T. Damour and V. F. Mukhanov, Phys. Lett. B **458**, 209 (1999) [arXiv: hep-th/9904075]; P. Creminelli, JCAP **0310**, 003 (2003) [arXiv:astro-ph/0306122]; N. Arkani-Hamed, P. Creminelli, S. Mukohyama and M. Zaldarriaga, JCAP **0404**, 001 (2004) [arXiv:hep-th/0312100]; M. Alishahiha, E. Silverstein and D. Tong, Phys. Rev. D **70**, 123505 (2004).

[5] T. J. Allen, B. Grinstein and M. B. Wise, Phys. Lett. B **197**, 66 (1987); L. A. Kofman and D. Y. Pogosian, Phys. Lett. B **214**, 508 (1988); D. S. Salopek, J. R. Bond and J. M. Bardeen, Phys. Rev. D **40**, 1753 (1989); A. D. Linde and V. F. Mukhanov, Phys. Rev. D **56**, 535 (1997) [arXiv:astro-ph/9610219]; P. J. E. Peebles, Astrophys. J. **510**, 523 (1999) [arXiv:astro-ph/9805194]; P. J. E. Peebles, Astrophys. J. **510**, 531 (1999) [arXiv:astro-ph/9805212].

[6] S. Mollerach, Phys. Rev. D **42**, 313 (1990); A. D. Linde and V. F. Mukhanov, Phys. Rev. D **56**, 535 (1997) [arXiv:astro-ph/9610219]; T. Moroi and T. Takahashi, Phys. Lett. B **522**, 215 (2001) [Erratum-ibid. B **539**, 303 (2002)] [arXiv:hep-ph/0110096]; D. H. Lyth and D. Wands, Phys. Lett. B **524**, 5 (2002) [arXiv:hep-ph/0110002]; D. H. Lyth, C. Ungarelli and D. Wands, Phys. Rev. D **67**, 023503 (2003) [arXiv:astro-ph/0208055]; K. Enqvist and S. Nurmi, JCAP **0510**, 013 (2005) [arXiv:astro-ph/0508573]; K. Ichikawa *et al.*, Phys. Rev. D **78**, 023513 (2008) arXiv:0802.4138 [astro-ph]; K. Enqvist and T. Takahashi, JCAP **0809**, 012 (2008) [arXiv:0807.3069 [astro-ph]]; A. L. Erickcek, M. Kamionkowski and S. M. Carroll, Phys. Rev. D **78**, 123520 (2008) [arXiv:0806.0377 [astro-ph]]; K. Enqvist and T. Takahashi, JCAP **0912**, 001 (2009) [arXiv:0909.5362 [astro-ph.CO]]; K. Enqvist, S. Nurmi, O. Taanila and T. Takahashi, JCAP **1004**, 009 (2010) arXiv:0912.4657 [astro-ph.CO]; A. L. Erickcek, C. M. Hirata and M. Kamionkowski, Phys. Rev. D **80**, 083507 (2009) [arXiv:0907.0705 [astro-ph.CO]].

[7] L. M. Wang and M. Kamionkowski, Phys. Rev. D **61**, 063504 (2000) [arXiv:astro-ph/9907431].

[8] S. Hannestad, T. Haugboelle, P. R. Jarnhus and M. S. Sloth, arXiv:0912.3527 [hep-ph].

[9] X. c. Luo, Astrophys. J. **427**, L71 (1994) [arXiv:astro-ph/9312004]; L. Verde *et al.*, Mon. Not. Roy. Astron. Soc. **313**, L141 (2000) [arXiv:astro-ph/9906301]; E. Komatsu and D. N. Spergel, Phys. Rev. D **63**, 063002 (2001) [arXiv:astro-ph/0005036].

[10] M. Kunz, A. J. Banday, P. G. Castro, P. G. Ferreira and K. M. Gorski, Astrophys. J. **563**, L99 (2001) [arXiv:astro-ph/0111250].

[11] W. Hu, Phys. Rev. D **64**, 083005 (2001) [arXiv:astro-ph/0105117].

[12] T. Okamoto and W. Hu, Phys. Rev. D **66**, 063008 (2002) [arXiv:astro-ph/0206155].

[13] G. De Troia et al. (for the BOOMERanG collaboration), MNRAS **343**, 284 (2003) [arXiv: astro-ph/0301294].

[14] N. Kogo and E. Komatsu, Phys. Rev. D **73**, 083007 (2006) [arXiv:astro-ph/0602099].

[15] D. M. Regan and E. P. S. Shellard, Phys. Rev. D **82**, 023520 (2010) [arXiv:1004.2915 [astro-ph.CO]].

[16] J. Smidt, A. Amblard, C. T. Byrnes, A. Cooray, A. Heavens and D. Munshi, Phys. Rev. D **81**, 123007 (2010) [arXiv:1004.1409 [astro-ph.CO]]; D. Munshi, P. Coles, A. Cooray, A. Heavens and J. Smidt, MNRAS **410**, 1295 (2011) [arXiv:1002.4998 [astro-ph.CO]]; J. Smidt, A. Amblard, A. Cooray, A. Heavens, D. Munshi and P. Serra, arXiv:1001.5026 [astro-ph.CO]; D. Munshi, A. Heavens, A. Cooray, J. Smidt, P. Coles and P. Serra, MNRAS **412**, 1993 (2011) [arXiv:0910.3693 [astro-ph.CO]].

[17] Q-G. Huang, JCAP **0905**, 005 (2009) [arXiv:0903.1542 [hep-th]]; C. T. Byrnes and G. Tasinato, JCAP **0908**, 016 (2009) [arXiv:0906.0767 [astro-ph.CO]]; D. Battefeld and T. Battefeld, JCAP **0705**, 012 (2007) [arXiv:hep-th/0703012]; D. Seery and J. E. Lidsey, JCAP **0701**, 008 (2007) [arXiv: astro-ph/0611034]; C. M. Peterson and M. Tegmark, [arXiv:1011.6675 [astro-ph.CO]]; F. Bernardeau and T. Brunier, Phys. Rev. D **76**, 043526 (2007) [arXiv:0705.2501 [hep-th]]; S. A. Kim, A. R. Liddle and D. Seery, Phys. Rev. Lett. **105**, 181302 (2010) [arXiv:1005.4410 [astro-ph.CO]]; N. Bartolo, E. Dimastrogiovanni, S. Matarrese and A. Riotto, JCAP **0911**, 028 (2009) [arXiv:0909.5621 [astro-ph.CO]].

[18] D. Langlois and T. Takahashi, JCAP **1102**, 020 (2011) [arXiv:1012.4885 [astro-ph.CO]]; E. Kawakami, M. Kawasaki, K. Nakayama and F. Takahashi, JCAP **0909**, 002 (2009) [arXiv:0905.1552 [astro-ph.CO]]; M. Sasaki, J. Valiviita and D. Wands, Phys. Rev. D **74**, 103003 (2006) [arXiv: astro-ph/0607627]; K. Enqvist and T. Takahashi, JCAP **0809**, 012 (2008) [arXiv:0807.3069 [astro-ph]].

[19] M-x. Huang and G. Shiu, Phys. Rev. D **74**, 121301 (2006) [arXiv: hep-th/0610235]; X. Gao and B. Hu, JCAP **0908**, 012 (2009) [arXiv:0903.1920 [astro-ph.CO]]; F. Arroja, S. Mizuno, K. Koyama, T. Tanaka, Phys. Rev. D **80**, 043527 (2009) [arXiv:0905.3641 [hep-th]]; S. Mizuno, F. Arroja, K. Koyama and T. Tanaka, Phys. Rev. D **80**, 023530 (2009) [arXiv:0905.4557 [hep-th]]; S. Renaux-Petel, JCAP **0910**, 012 (2009) [arXiv:0907.2476 [astro-ph.CO]]; S. Mizuno, F. Arroia and K. Koyama, Phys. Rev. D **80**, 083517 (2009) [arXiv:0907.2439 [hep-th]]; Q-G. Huang, JCAP **1007**, 025 (2010) [arXiv:1004.0808 [astro-ph.CO]]; K. Izumi and S. Mukohyama, JCAP **1006**, 016 (2010) [arXiv:1004.1776 [astro-ph.CO]].

[20] M. Hindmarsh, C. Ringeval and T. Suyama, Phys. Rev. D **81**, 063505 (2010) [arXiv:0911.1241 [astro-ph.CO]]; D. M. Regan and E. P. S. Shellard, Phys. Rev. D **82**, 063527 (2010) [arXiv:0911.2491 [astro-ph.CO]]; C. Ringeval, Adv. Astron. **2010**, 380507 (2010) [arXiv:1005.4842 [astro-ph.CO]].

[21] E. Komatsu *et al.* [WMAP Collaboration], Astrophys. J. Suppl. **148**, 119 (2003) [arXiv:astro-ph/0302223]; E. Komatsu *et al.* [WMAP Collaboration], Astrophys. J. Suppl.

180, 330 (2009) [arXiv:0803.0547 [astro-ph]]; E. Komatsu *et al.* [WMAP Collaboration], Astrophys. J. Suppl. **192**, 18 (2011) [arXiv:1001.4538 [astro-ph.CO]].

[22] N. Dalal, O. Dore, D. Huterer and A. Shirokov, Phys. Rev. D **77**, 123514 (2008) [arXiv:0710.4560 [astro-ph]]; A. Slosar, C. Hirata, U. Seljak, S. Ho and N. Padmanabhan, JCAP **0808**, 031 (2008) [arXiv:0805.3580 [astro-ph]]; S. Matarrese and L. Verde, Astrophys. J. **677**, L77 (2008) [arXiv:0801.4826 [astro-ph]]; C. Carbone, L. Verde and S. Matarrese, Astrophys. J. **684**, L1 (2008) [arXiv:0806.1950 [astro-ph]]; J. Q. Xia, M. Viel, C. Baccigalupi, G. De Zotti, S. Matarrese and L. Verde, Astrophys. J. **717**, L17 (2010) [arXiv:1003.3451 [astro-ph.CO]]; J. Q. Xia, A. Bonaldi, C. Baccigalupi, G. De Zotti, S. Matarrese, L. Verde and M. Viel, JCAP **1008**, 013 (2010) [arXiv:1007.1969 [astro-ph.CO]]; L. Verde and S. Matarrese, Astrophys. J. **706**, L91 (2009) [arXiv:0909.3224 [astro-ph.CO]]; F. Schmidt and M. Kamionkowski, Phys. Rev. D **82**, 103002 (2010) [arXiv:1008.0638 [astro-ph.CO]].

[23] P. A. R. Ade *et al.* [Planck Collaboration], [arXiv:1101.2022 [astro-ph.IM]].

[24] P. Creminelli and M. Zaldarriaga, JCAP **0410**, 006 (2004) [arXiv:astro-ph/0407059].

[25] R. Keisler *et al.* (for the SPT collaboration), Astrophys. J. **743**, 28 (2011) [arXiv: 1105.3182 [astro-ph.CO]].

[26] K. M. Smith, M. LoVerde and M. Zaldarriaga, Phys. Rev. Lett. **107**, 191301 (2011) [arXiv:1108.1805 [astro-ph.CO]].

[27] D. Babich and M. Zaldarriaga, Phys. Rev. D **70**, 083005 (2004) [arXiv:astro-ph/0408455].

[28] P. Creminelli, L. Senatore and M. Zaldarriaga, JCAP **0703**, 019 (2007) [arXiv:astro-ph/0606001].

[29] T. L. Smith, M. Kamionkowski and B. D. Wandelt, Phys. Rev. D **84**, 063013 (2011) [arXiv:1104.0930 [astro-ph.CO]].

[30] L. Boubekeur and D. H. Lyth, Phys. Rev. D **73**, 021301 (2006) [arXiv:astro-ph/0504046].

[31] A. L. Erickcek, S. M. Carroll and M. Kamionkowski, Phys. Rev. D 78, 083012 (2008) [arXiv:astro-ph/0808.1570].

[32] N. Joshi, A. Rotti and T. Souradeep, Phys. Rev. D **85**, 043004 (2012) [arXiv:1109.0729 [astro-ph.CO]].